THE PUBLISHING HOUSE
OF THE ROMANIAN ACADEMY

PROCEEDINGS OF THE ROMANIAN ACADEMY, Series A,
Volume 22, Number 3/2021, pp. 255–264

STRUCTURAL INVESTIGATIONS ON THE PROGRESSIVE COLLAPSE OF A STEEL-TIMBER INTERMEDIATE ROOFING

Calin NEAGU[1], Dan DUBINA[1,2], Florea DINU[1,2], Ioan PETRAN[3]

[1] Politehnica University Timisoara, CMMC Department, Timisoara, Romania
[2] Romanian Academy, Timisoara Branch, CCTFA Research Centre, Timisoara, Romania
[3] Technical University of Cluj Napoca, Department of Structures, Cluj Napoca, Romania
Corresponding author: Ioan PETRAN, E-mail: ioan.petran@dst.utcluj.ro

Abstract. Building constructions are susceptible to significant risks from numerous low probability hazards during their design lifetime. Typical examples include fire, impact, explosion, earthquake, and severe weather hazards (wind, snow). The probable risks also include a special category pertaining to unidentifiable events, such as human errors in design and construction. As such exposures and hazards are difficult to quantify, the consequences can be severe, ranging from injuries or loss of life to serious economic costs. The paper presents the results of investigations conducted in the aftermath of a partial collapse during the construction of an intermediate roof built from hybrid steel-timber trusses in an existing market. The experimental tests and numerical simulations allowed the investigators to reconstruct the chain of events and identify the local damage that triggered the progressive collapse.

Key words: steel-timber truss, construction error, accidental collapse, experimental testing, forensic investigation.

1. INTRODUCTION

Numerous low probability hazards can pose a significant risk to the structural integrity of a construction during its lifetime, ranging from local damage or failure to complete structural collapse. Typical examples include high intensity fire, impact, explosion, earthquake, and severe weather hazards (wind, snow). Therefore, the probability of occurrence and the intensity of such extreme loading conditions must be taken into account to ensure the service safety of construction. Thus, well designed constructions are expected to survive accidental loading events by limiting the extent of damage and preventing the development of progressive collapse [1, 2, 3, 4, 5, 6]. Besides the ones mentioned above, a special category of risk pertains to unidentifiable events, such as human errors in design and construction [7, 8, 9]. Because exposure and hazard are difficult to quantify in such cases, the consequences can be severe, ranging from injuries or loss of life to serious economic costs. For example, investigations in recent failures of roof structures (constructed with steel or timber) in Europe during winters with high snow loading have indicated instability as a common/predominant failure mode [10]. However, subsequent investigations indicated that the level of snow loading rarely exceeded the values used during the design of the structures in question; instead, the most important cause of failure was frequently observed to be human error. The following two cases are representative in order to describe the consequences of such accidental failures. First is the collapse of an ice-arena timber roof in Bad Reichenhall on the 2nd of January 2006 under the effect of snow [11], when 15 people died and 30 people were injured. The technical report concluded that the load intensity was significant but not exceeding the design snow load, and the collapse was not due to a single cause, but rather a series of defects and damages (e.g. flaws in design, poor quality control). Then, in less than a month, the collapse of Katowice Fair Building in Poland on the 28th of January 2006, which caused 65 fatalities and heavy injuries to 130 people [12]. Also, in this case, the collapse was caused by a combination of wrong constructional solution, insufficient strength and stiffness of structural elements but also some overloading action due to thick ice – snow layer. Note that in January 2002 the roof of the building was repaired due to a

local collapse. Faulty materials, systems, or fabrication processes end in vulnerable structures, and, as a result, even moderate intensity loadings can become catastrophic. Besides, even with comprehensive inspections, a few defects may remain undetected and therefore pose a risk to safety during erection or later during operations.

The paper presents the results of investigations conducted following partial collapse during the construction of an intermediate roof in an existing market in Timisoara [13]. The structure, spanning 20.40 m, was built with truss beams realized from glued laminated timber and steel ties. The accident occurred during erection and affected two already assembled beams. Post accident, material samples and assemblies were extracted from an existing undamaged beam and tested experimentally. Then, numerical models were calibrated against the tests and further used to simulate the collapse and reveal the chain of events that led to the accident.

2. STRUCTURAL DESCRIPTION

The structure under investigation was a new intermediate roof being built inside an existing open-air market located in Timisoara, Romania (see Fig. 1). This intermediate roof was designed to protect the commercial space from severe weather conditions. The roof, constructed with glued laminated timber beams and steel posts and ties (Fig. 2), partially collapsed during the erection phase when a transversal beam fractured and resulted in the failure of the adjacent beam (see Fig. 1). The beams, with a total span of 20.40 m, comprised five sections joined on-site with a hybrid timber-steel bolted connection (see Fig. 3). The supports at both the beam ends were pinned. The beam sections, denoted as T1 to T5, were of almost equal length (T1, T5 = 4.05 m; T2, T3, T4 = 4.10 m). Each beam section contained two individual beams (pair section), each 5 cm thick, joined at each splice connection. The timber beam was a symmetrical double-pitched beam with the following dimensions:

- T1, T5: height varied from 25 cm at the outer end to 29 cm at the inner end;
- T2, T4: height varied from 29 cm at the outer end to 33.50 cm at the inner end;
- T3: height varied from 33.50 cm at both ends to 35.50 cm in the middle section.

The beam sections were joined using double-shear steel-to-timber and timber-to-timber connections made of M12 bolts class 8.8 and 5×20 cm timber elements (called link elements) with a length of 1.0 m between T1-T2 and 1.20 m between T2-T3 and T3-T4. The steel posts had two welded gussets of 10 mm thickness each at the top (Fig. 4a). Intermediately, the twin beam sections were connected using 5×20 and 30 cm long timber elements, which also served to support the top brackets used to fix the purlins. Although both the link elements and the timber beams were originally designed to be built with oak wood, the solution was subsequently changed to glued laminated timber elements. Ties were made from round steel bars with a diameter of 20 mm while the posts were built with 50×50×5 mm square tubes. To allow tightening, the ties were threaded at both the beam ends and supplied with nuts and washers. All the steel elements were composed of S235 JR steel (EN 10025-2). The beam splicing was configured so that only one bolt row connected the timber sections through the gusset plates (Fig. 4b).

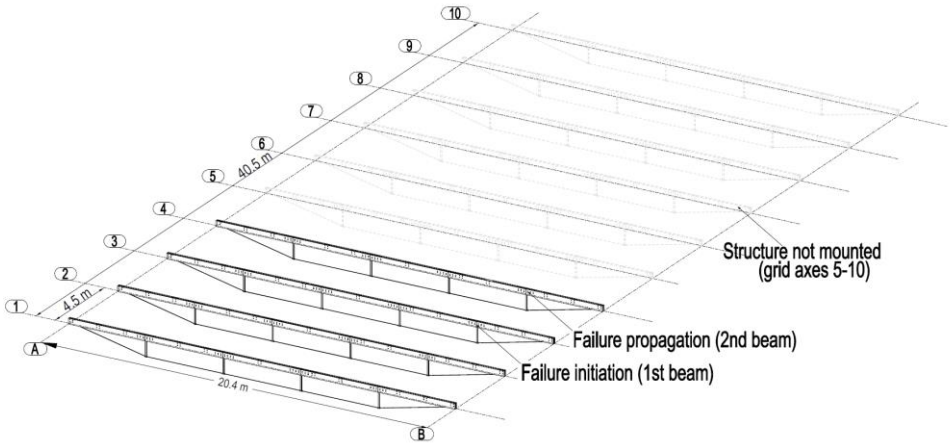

Fig. 1 – 3D view of the intermediate roof structure.

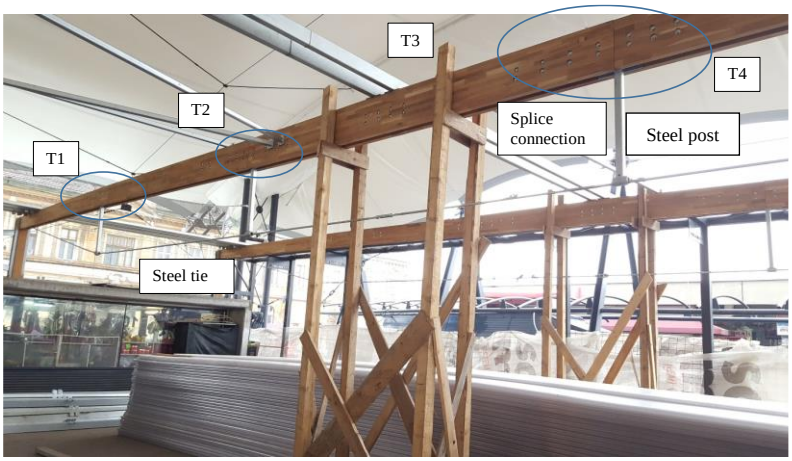

Fig. 2 – View of the first two beams (axis 1, axis 2) with the temporary supporting structures still in position.

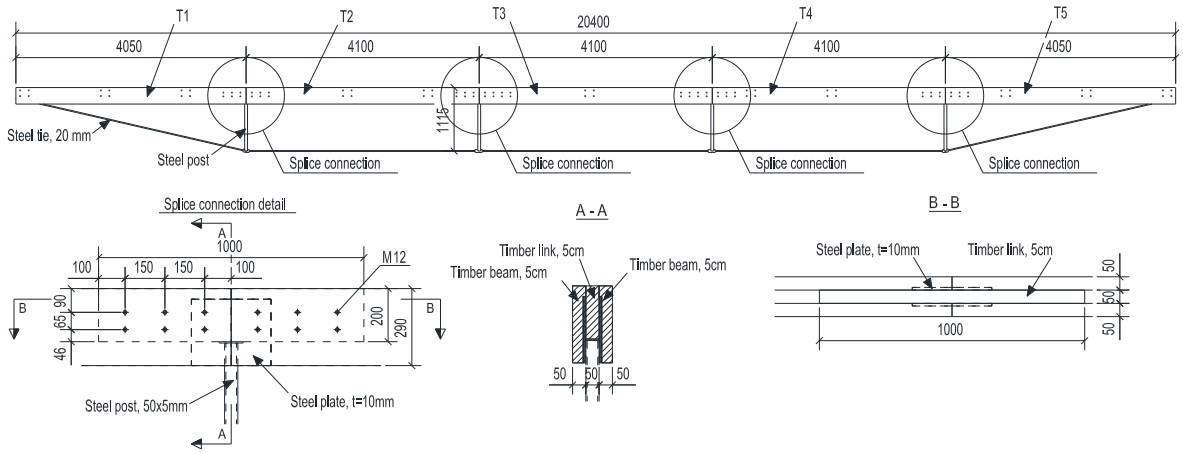

Fig. 3 – Geometry of the beam and fabrication details.

a) b)

Fig. 4 – Splice connection: a) steel post with link steel and timber elements; b) beam ready for erection.

The mechanical properties of the timber structure were determined experimentally at Urban Incerc Timişoara (2017) (notations are according to [2]):

– Density, $\rho = 751.37$ kg/m^3 (mean value);

– Elastic modulus parallel to the fibers, $E_{m,g} = 16.0$ kN/mm^2 (minimum value);

– Compressive strength parallel to the fibers, $f_{c,0} = 63.02$ N/mm^2 (average value);

– Bending resistance parallel to the fibers, $f_{m,0,l,k} = 53.60$ N/mm^2 (minimum value).

Moreover, the assembly between the threaded bar and the nut was tested for tension in the same test program (three specimens were tested in total). According to the test results and the observations made during testing, the large tolerances in the nuts reduced the ultimate resistance of the assembly from a nominal value of 73.42 kN to a maximum force in the threaded rods of 13.38 kN, 25.85 kN, and 37.44 kN.

3. ROOF FAILURE

3.1. Description of the accident

The accident occurred during construction stage, when a transversal beam completely collapsed and fell from the end supports. The falling beam led to the failure of an adjacent beam, similar to a domino effect. The investigation that followed aimed to find the causes of the accident and conditions necessary for the project to be completed while retaining the original design and structural elements with or without any retrofitting interventions.

During a visit at the construction site after the accident, sections of the beam that initially failed were identified and assembled to reconstruct the beam (Fig. 5a). The reconstruction revealed that the fracture had occurred at the splice connection between sections T1 and T2 of the beam (see Fig. 6 for identification of the beam sections). There was no evidence of any damaged or broken link. However, one such element was identified as the most probable part of the failed connection, as it exhibited localized tear-out damage in the first row of bolts (Fig. 5b).

a) b)

Fig. 5 – Two sections of the beam reconstructed after the failure: a) view with the elements on the ground; b) connecting device with the post, two gusset plates, and timber link element.

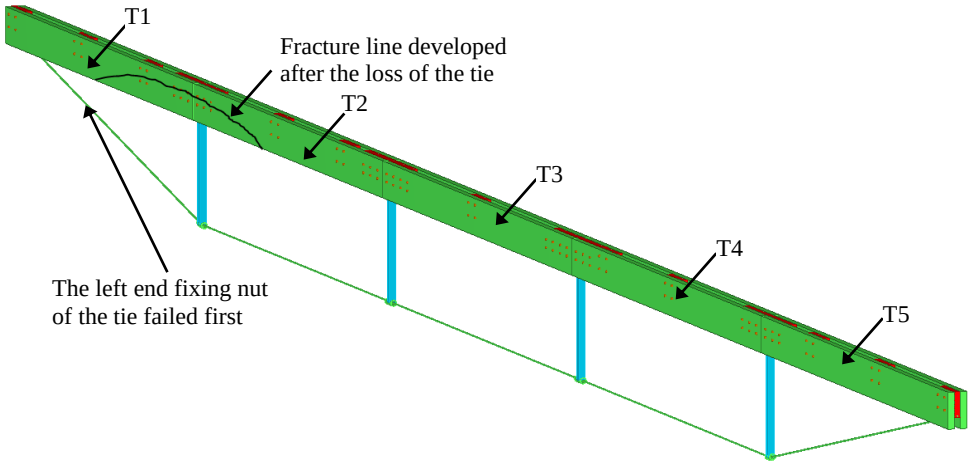

Fig. 6 – The initiation of collapse in beam from axis 3, between section T1 and T2 (the fracture line is also sketched).

3.2. Experimental testing

Four specimens, each comprising two beam sections, the post, and the connecting link, were extracted from an existing beam that was not mounted at the time of the accident, two from each side of the beam. The first two specimens, denoted S1 and S2, were extracted from the T1-T2 and T4-T5 connections and the other two from the T2-T3 and T3 -T4 connections (denoted S3 and S4). The specimens had a length of 4.05 m and

two spans, 2.85 m and 1.20 m, respectively. For specimens S1 and S2, the load was applied on top of the post (Fig. 7a), whereas it was applied with an eccentricity *e* of 0.35 m for S3 and S4 (Fig. 7b). The different loading setup aimed at evaluating the possible effects of bending/shear ratio on the peak capacity and failure mode.

The vertical load was applied quasi-statically using a displacement control protocol and was gradually increased until the failure of the test specimens (Fig. 8a). The amplitude of the load was monitored using the load cell of the actuator. The instrumentation used during testing comprised two main components, namely, displacement transducers and a digital image correlation system produced by Correlated Solutions, Inc. (VIC-3D) [14] (Fig. 8b).

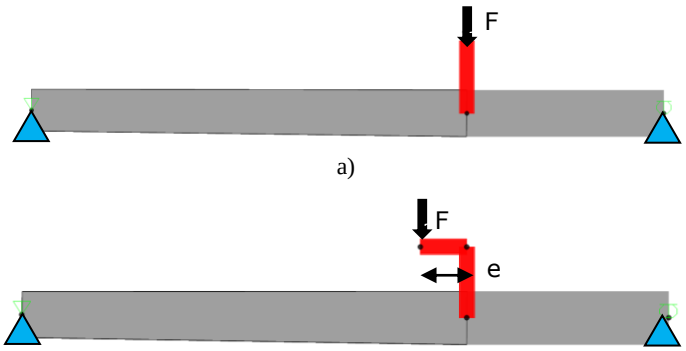

Fig. 7 – Loading setup for experimental testing: a) specimens S1, S2; b) specimens S3, S4.

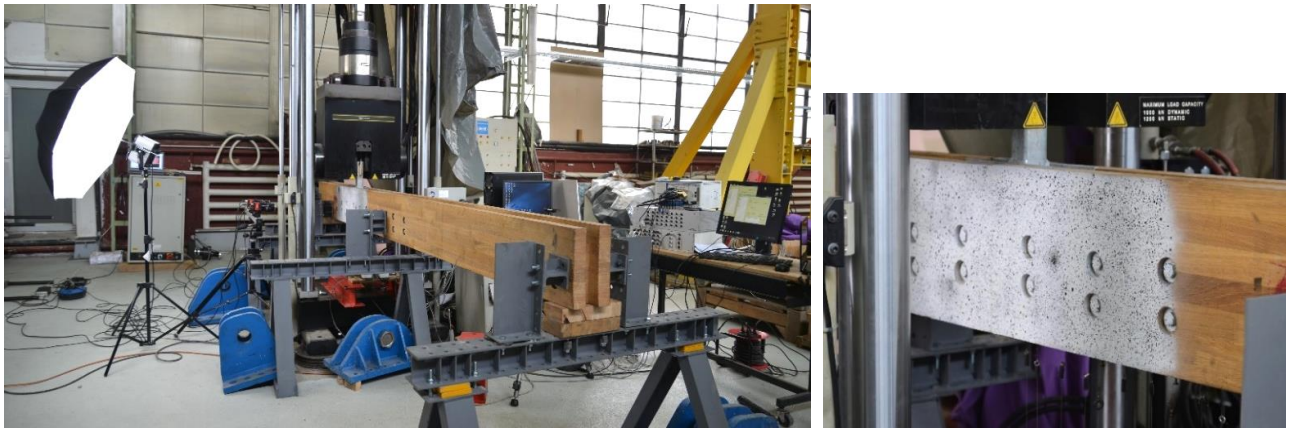

a) b)

Fig. 8 – View from laboratory: a) test setup and specimen ready for testing; b) surface preparation for VIC-3D measurements.

Fig. 9a shows the force-displacement curves for specimens S1 and S2, while Fig. 10 shows the failure mode for the same specimens. In case of specimen S1, a partial failure (most probably a partial split of the timber link) was observed at a force equal to 24.4 kN, where it dropped to 13.10 kN. Subsequently, the capacity increased until the final fracture of the link element owing to a complete split at a maximum force of 30.5 kN (Fig. 10a). This failure mode, also called “zip-effect”, appears when a splitting-failure of one fastener makes the subsequent fasteners in a row to fail. The bending moment at the maximum applied force was 25.10 kNm. Only a partial longitudinal crack was observed in the upper area of the beam elements because of compression, a crack that propagated longitudinally up to the second bolt row. It is also visible in the figure that the deformation of the bolts is larger in the second bolt row from the right-hand area, indicating an uneven transfer of shear loads within the hybrid steel-timber connection. In case of specimen S2, the peak applied force was 29.70 kN, very close to that obtained for specimen S1, and the corresponding bending moment was 24.40 kNm. The splitting of the link element within the larger span caused the failure as shown in Fig. 10b. Only partial cracks developed in the upper area of the beam upon compression.

Specimens S3 and S4 were tested by eccentrically applying an increasing vertical force (eccentricity e = 0.35 m). Fig. 9b shows the force-displacement curves for the two specimens. In case of specimen S3, the

cracks first initiated in the upper compressed area of the beam, which then propagated up to the second bolt row; however, they did not cause a significant decrease in the beam capacity. The failure was produced owing to the splitting of the beam from the larger span (Fig. 11a). The maximum force was 31.6 kN, after which the capacity dropped sharply to 20 kN. The test was terminated when the vertical displacement reached 78 mm. The maximum bending moment was 33.80 kNm. No cracks were observed in the link element. As the fracture developed in the beam elements and not in the link, it was possible to observe the initiation and propagation of the cracks in the connection up to the failure point. Thus, the initiation started inside the beam, between the second and the third bolt row, after which it propagated beyond the second bolt row and finally the failure was caused by the beam splitting, as seen in Fig. 12. In case of specimen S4, the first crack formed in the upper compressed area of the beam, which then propagated up to the second bolt row; however, it did not produce a significant decrease in the beam capacity. Splitting of the link element from the larger span for almost half the length caused the failure, as seen in Fig. 11b. The maximum force value was 32.9 kN, after which the capacity dropped sharply, and the test was terminated. The maximum bending moment was 35.2 kNm.

Table 1 summarizes the peak force applied in each test and the corresponding maximum bending moment. Notably, three specimens (S1, S2, S4) failed owing to the splitting of the link element, while the failure of specimen S3 was caused by the splitting of the beam. However, the maximum applied forces were very similar, indicating that the resistance of the beam matches very closely with that of the link element. Therefore, the bearing capacity of the joint can be increased only by increasing the capacities of both the beams and link elements.

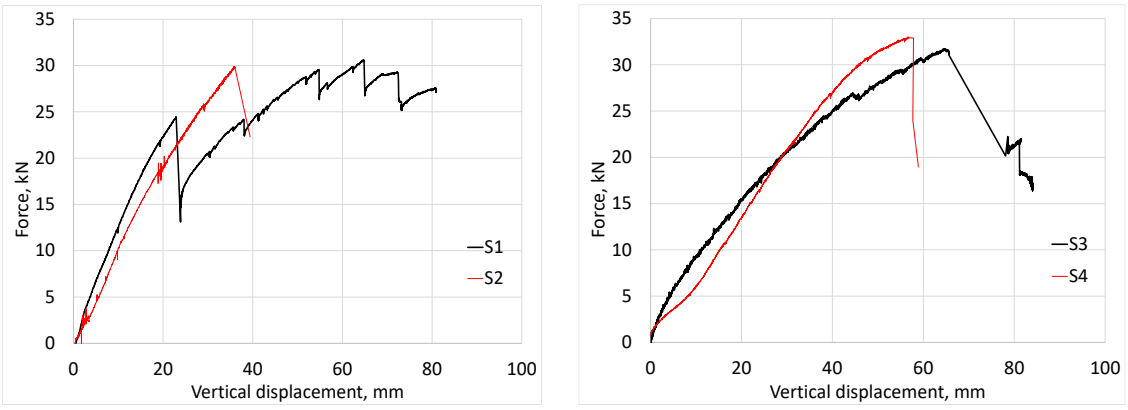

a) b)

Fig. 9 – Experimental force-displacement curves: a) specimens S1, S2; b) specimens S3, S4.

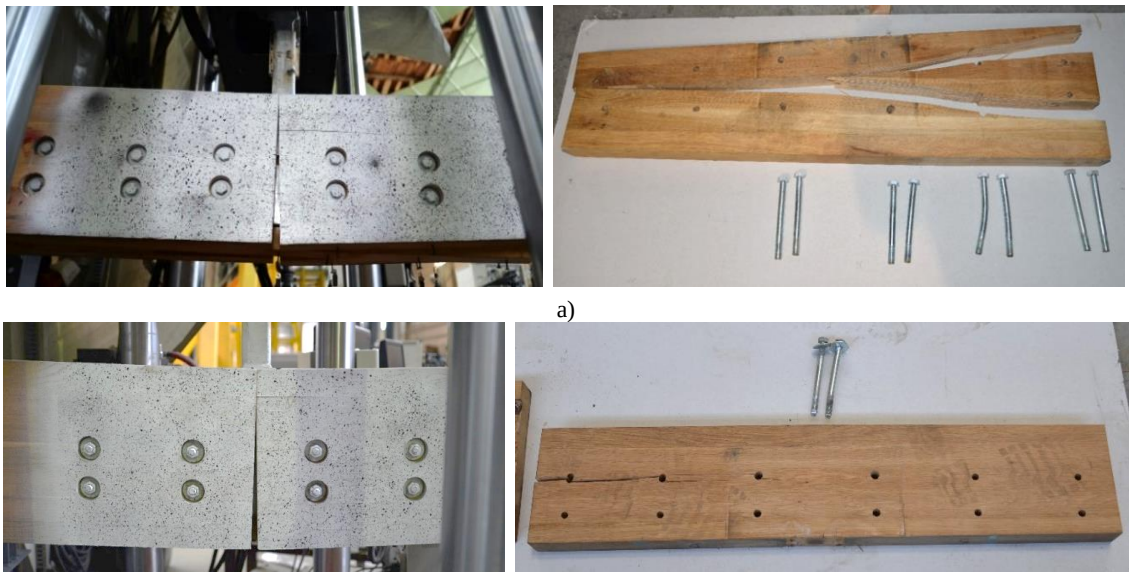

a)

b)

Fig. 10 – Failure mode: a) specimen S1; b) specimen S2.

a)

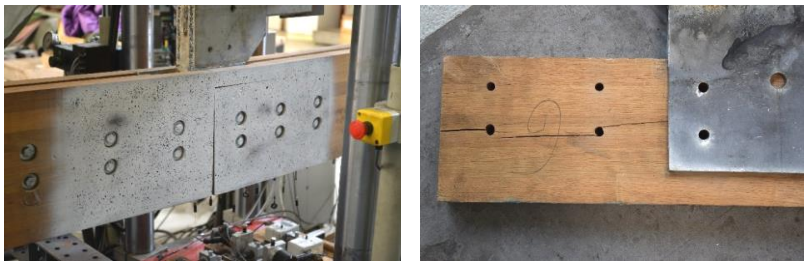

b)

Fig. 11 – Failure mode: a) specimen S3; b) specimen S4.

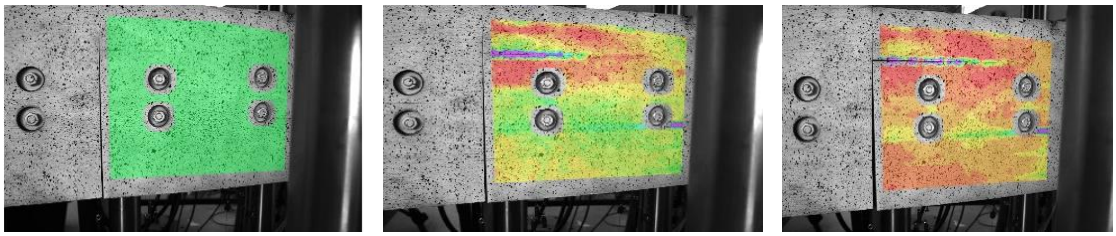

1 2 3

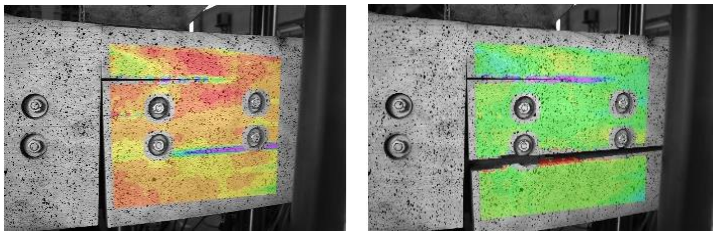

4 5

Fig. 12 – Initiation and development of cracks measured with VIC-3D system, specimen S3 (from 1 to 5).

Table 1

Maximum applied force and bending moment for specimens S1-S4

Specimen	F_{max} [kN]	M_{max} [kNm]
S1	30.5	25.1
S2	29.7	24.4
S3	31.6	33.8
S4	32.9	35.2
Mean value	31.05	29.45
Minimum value	29.07	24.4

3.3. Numerical investigations on the causes of collapse

Numerical analyses were performed to evaluate the load bearing capacity of the beam assembly to identify the potential flaws in design and construction that caused the collapse. Numerical models for the connections were first constructed and calibrated based on the experimental results, using SAP2000 program [15]. The geometrical and material properties and the loading schemes complied with the laboratory conditions and the properties of the materials that were evaluated with experimental testing. Two types of frame hinges

were assigned to the beam sections, that is, shear V2 and moment M3, both uncoupled. Figure 13 shows the comparative force-displacement curves in the nonlinear static analysis and experimental testing. The numerical models accurately estimated the initial stiffness, maximum force, and corresponding maximum displacement.

To determine the distribution of forces in the beam, a complete model of the beam assembly was obtained by integrating the joint models (Fig. 14a). The geometric and material characteristics were obtained from the technical project and the test report provided by Urban Incerc Timisoara (2017). Considering that the beam was not loaded with any imposed load at the time of collapse, the beam was first analyzed for the effects of gravity load caused by the self-weight of the beam assembly, which was then increased by 50% to account for possible deviations from the nominal weight and other materials/tools used during the construction stage. A static analysis was applied to determine the maximum values of forces and bending moments in the timber elements, steel post, and ties at the time of failure. As can be seen from Fig. 14b, the values of the bending moment and shear force are lower than the peak values recorded during experimental testing, which eliminates them as the source of failure. However, the axial force, which amounts to 19.89 kN, is higher than the minimum resistance measured for the threaded rods (13.38 kN). In these conditions, the failure most probably initiated from the steel tie, which failed suddenly in tension under the effect of the gravity load. To investigate the removal effect on the structure, a two-stage analysis was performed to assess if the complete structural collapse was triggered by the failed tie. In the first stage, the gravity load (multiplied by a safety factor of 1.5) was applied to the structure. In the second stage, the tie was removed almost instantly (Δt = 0.001 s). The response of the remaining structure was then evaluated using a non-linear dynamic time history analysis.

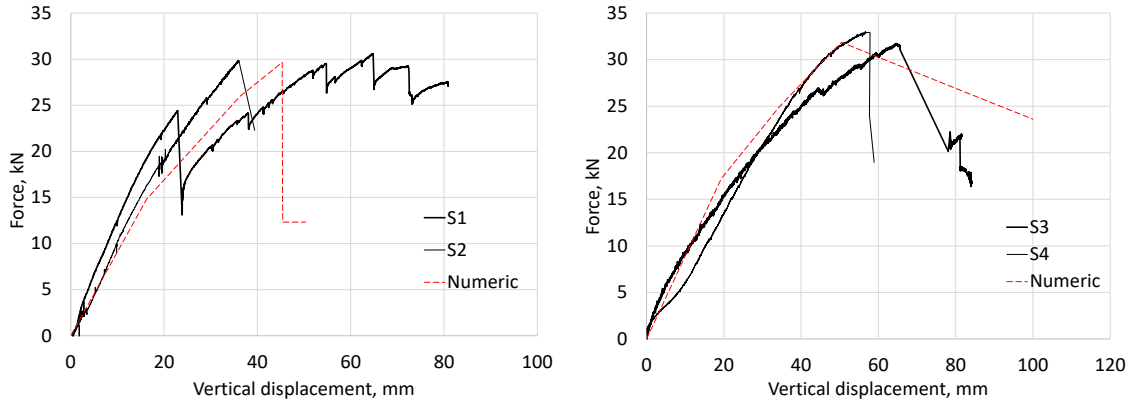

Fig. 13 – Force-displacement curves, experimental vs. numeric: a) specimens S1, S2; b) specimens S3, S4.

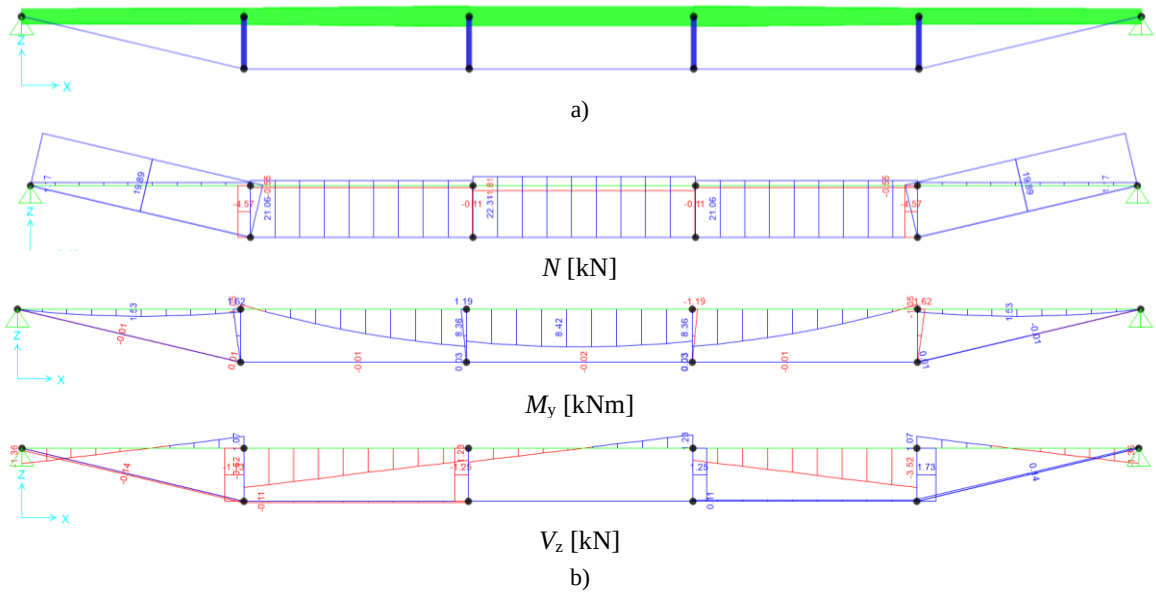

Fig. 14 – Hybrid timber-steel beam model in SAP2000: a) complete beam model; b) axial force, in-plane bending moment M_y, and shear force V_z under gravity loads due to self-weight.

As seen from Fig. 15a, after the tie is lost, the timber beam alone cannot support the applied gravity loads and fails at the first intermediate splice. Notably, the same point of fracture was identified on the site (Fig. 5a). Moreover, the instantaneous removal of the tie exposed the structure to a dynamic effect, and thus much greater loads were imposed on the structure. For comparison, Fig. 15b shows the deformed shape of the beam in the case of a quasi-static removal of the tie. Even when the vertical deflection reaches 148 mm, the bearing capacity of the connections is not exceeded, and the failure is prevented.

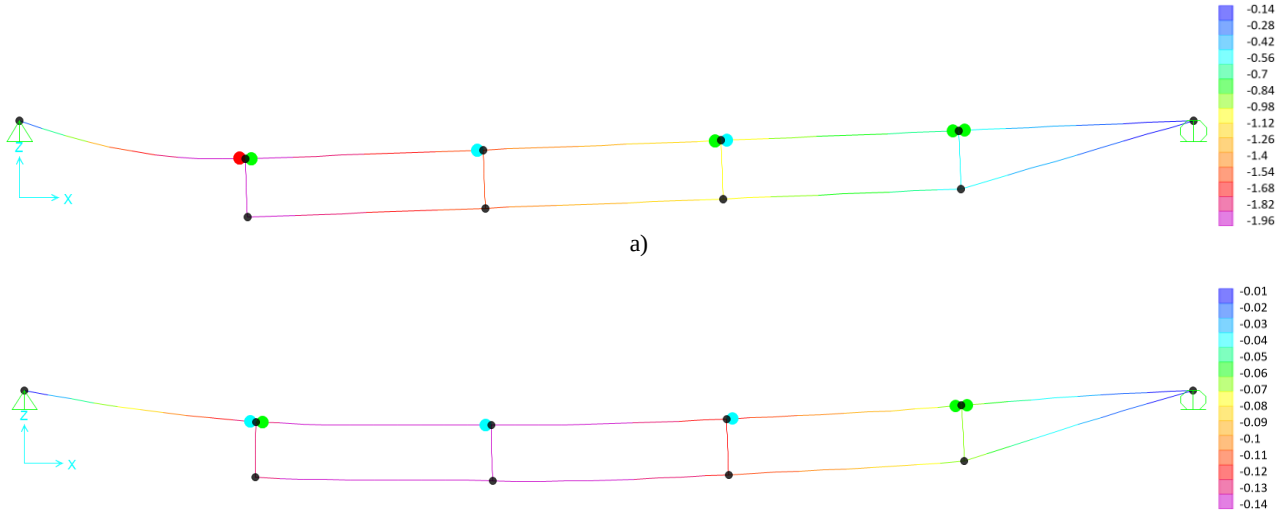

Fig. 15 – Deformed shape of the beam and distribution of plastic hinges in splice connections: a) removal time Δt = 0.001 s; b) quasi-static removal (the scale indicates the vertical deflection, in m).

4. CONCLUSIONS

Structural failures can initiate from various sources, including severe hazards and human error in design and construction. Other potential sources include faulty materials, systems, or fabrication processes used in a project. Even with comprehensive inspections, certain defects may remain undetected and therefore pose a significant safety risk during erection or later, during the operations. The case study presented in the paper described the investigation of possible factors contributing to the collapse of an intermediate roof erected inside an existing open-air market. The hybrid steel-timber truss structure of the roof was under erection at the time of collapse, with no other load than its self-weight and a few additional loads from materials/tools used during the construction stage. The collapse took place without any warning; therefore, little information was available about the chain of events and possible triggering factor. The tests on the materials and components allowed the investigators to evaluate the behavior of timber and steel elements, including the complex beam splice connection. The subsequent construction of a full-scale numerical model and dynamic analysis revealed the weakest component that initially failed and the progression of damages that ultimately led to the accidental collapse. Based on these facts, the following remarks and recommendations can be suggested:

– The structure under investigation cannot be mounted without extensive verifications, repairing works, and possibly replacement of entire sections.

– The use of different materials (i.e., timber, steel) in a structure requires careful consideration in design. This is especially important when the load is shared and/or transferred between elements constructed with these different materials.

– Connections generally include a complex stress state. In case of timber connections, there are additional factors that aggravate this stress, for example, wood anisotropy and the presence of stresses perpendicular to the grain. Therefore, the accurate modeling of such connections must take into account the relevant parameters, and where possible, experimental data may be used to validate the model.

– Careful consideration should be given to control during execution and construction. In most cases, failures occur due to gross human errors.

– To reduce the risk of progressive collapse and brittle fracture, systems should possess adequate continuity, redundancy, and ductility.

– For elements with no redundancy, for example trusses with tension ties, the connections of the elements should be designed with overstrength (to develop the full axial strength of the element).

REFERENCES

1. EN 1990, *Eurocode 0: Basis of Design*, European Committee for Standardisation, Brussels, CEN, 2002.
2. EN 1995-1-1. *Educational Materials for Designing and Testing of Timber Structures – TEMTIS. Handbook 2 – Design of timber structures according to Eurocode 5*, Leonardo da Vinci Pilot Project, 2008.
3. *Design of Buildings to Resist Progressive Collapse*, Department of Defense DoD, 2016.
4. F. DINU, I. MARGINEAN, D. DUBINA, I. PETRAN, *Experimental testing and numerical analysis of 3D steel frame system under column loss*, Eng. Struct., **113**, pp. 59–70, 2016, doi: 10.1016/j.engstruct.2016.01.022.
5. M. TOHIDI, C. BANIOTOPOULOS, *Effect of floor joint design on catenary actions of precast floor slab system*, Eng. Struct., **152**, pp. 274–288, 2017, doi: 10.1016/j.engstruct.2017.09.017.
6. S. GERASIMIDIS, C.C. BANIOTOPOULOS, *Disproportionate collapse analysis of cable-stayed steel roofs for cable loss*, Int. J. Steel Struct., **11**, *1*, pp. 91–98, 2011, doi: 10.1007/S13296-011-1008-4.
7. B.R. ELLINGWOOD, R. SMILOWITZ, D.O. DUSENBERRY, D. DUTHINH, H.S. LEW, N.J. CARINO, *Best practices for reducing the potential for progressive collapse in buildings*, National Institute of Standards and Technology, Gaithersburg, MD, NIST IR 7396, 2007, doi: 10.6028/NIST.IR.7396.
8. A. KLASSON, I. BJÖRNSSON, R. CROCETTI, E.F. HANSSON, *Slender roof structures – Failure reviews and a qualitative survey of experienced structural engineers*, Structures, **15**, pp. 174–183, 2018, doi: 10.1016/j.istruc.2018.06.009.
9. H.P. HONG, W.X. HE, *Effect of human error on the reliability of roof panel under uplift wind pressure*, Struct. Saf., **52**, pp. 54–65, 2015, doi: 10.1016/j.strusafe.2014.07.001.
10. E. FRÜHWALD HANSSON, *Analysis of structural failures in timber structures: Typical causes for failure and failure modes*, Engineering Structures, **33**, *11*, pp. 2978–2982, 2011, doi: 10.1016/j.engstruct.2011.02.045.
11. S. WINTER, H. KREUZINGER, *The Bad Reichenhall ice-arena collapse and the necessary consequences for wide span timber structures*, **4**, pp. 1978–1985, 2008.
12. A. BIEGUS, K. RYKALUK, *Collapse of Katowice fair building*, Engineering Failure Analysis, **16**, *5*, pp. 1643–1654, 2009, doi: 10.1016/j.engfailanal.2008.11.008.
13. D. DUBINA, F. DINU, C. NEAGU, *Evaluarea soluției tehnice și a siguranței în exploatare a structurii acoperișului intermediar al Pieței Badea Cârțan din Timișoara*, AICPS Review, **1-2**, pp. 44–52, 2019.
14. *VIC-3D Digital Image Correlation Software*, Correlated Solutions Inc, 2016.
15. *Structural Software for Analysis and Design | SAP2000*, Computers and Structures, Inc. (CSI), Walnut Creek, CA 94596 USA.

Received April 7, 2021